Title

Vaporization behavior of Ir4(CO)12 and Re2(CO)10 measured by torsion effusion gravimetric method

Authors

Chandra, Dhanesh
Lau, KH
Nforbi, Lum-Ngwegia Ngwa
et al.

Publication Date

2021-12-01

DOI

10.1016/j.tca.2021.179068

Peer reviewed

Vaporization Behavior of $Ir_4(CO)_{12}$ and $Re_2(CO)_{10}$ Measured by Torsion Effusion Gravimetric Method

Dhanesh Chandra[1]*, Anjali Talekar[1], K.H. Lau[2], Raja Chellappa[3], Wen Ming Chien[1], Jeffry Urban[4], Tevye R. Kuykendall[4]

[1]Chemical and Materials Engineering, MS388, University of Nevada, Reno, Reno, NV 89557

[2]SRI International, 333 Ravenswood Ave., Menlo Park CA 94025

3. Los Alamos National Laboratory, Los Alamos New Mexico

4. Molecular Foundry, Lawrence Berkeley national laboratory CA

*Corresponding Author's e-mail: dchandra@unr.edu

Abstract

Metal carbonyls are of great importance in chemical vapor deposition (CVD), composite materials fabrication, and other near-net shape technologies. Carbonyl CVD application applies to deposition of high-purity metallic/alloy coatings for which vapor pressure data is essential. The vapor pressure data is used for many low and high temperature CVD applications. In this study, we report vapor pressures of solid $Ir_4(CO)_{12}$ and $Re_2(CO)_{10}$ carbonyls, measured by using the Knudsen Cell methodology with a torsion effusion gravimetric system. The equilibrium total vapor pressure determined is given by the equation, $P_{e\ Ir4(CO)12}$ (kPa) = 12.6 - 6615/T(K). The solid $Ir_4(CO)_{12}$ exhibited incongruent vaporization, with ~ 66% conversion from a tetramer to metallic iridium, according to $Ir_4(CO)_{12}(s) \rightarrow Ir(s)+12CO$, as suggested by differences in the measured and theoretical molecular weights of the vaporizing species of 128 g/mol and 1105 g/mol, respectively. The $Re_2(CO)_{10}$ on the other hand, showed congruent vaporization, $Re_2(CO)_{10}$ (s) = $Re_2(CO)_{10}$ (g) in the temperature range of measurements. The equilibrium total vapor pressure determined is given by the equation, $P_{e\ Re2(CO)10}$ (kPa) = 9.396- 4167/T(K). We measured a molecular weight of 675 g/mol whereas the theoretical value is 625 g/mol In both cases we used Whitman-Motzfeldt methodology to obtain equilibrium vapor pressures. The total vapor pressures of these carbonyls, partial pressures of gas species, average molecular weights of the effusing gases, equilibrium constants for the vaporization reactions, their enthalpies, entropies, and Gibbs energies of the Ir and Re carbonyls as well comparison of vaporization thermodynamics with other carbonyls from Group VIA to VIIIA are presented in this paper.

Keywords: Vaporization Thermodynamics, Metal Carbonyls, Torsion effusion method, CVD

1. Introduction.

Metal carbonyls have important applications in the chemical vapor deposition (CVD) of metals and alloys, fabrication of composite materials, and other technologies [1]. Chandra et al. [2,3] and Shorovshrov et al. [4,5], reported depositing metallic coating on fibers. Vaporization thermodynamics of metal carbonyls are important for CVD processes [1,6]. Vapor pressure measurement s have been made on metal carbonyls such as, $Ni(CO)_4$, $Fe(CO)_5$, $Cr(CO)_6$, $W(CO)_6$, $Os_3(CO)_{12}$, $Co_2(CO)_8$, $Mo(CO)_6$, $Re_2(CO)_{10}$, $Mn(CO)_5$, $Rh_6(CO)_{16}$, and $Ru_3(CO)_{12}$ and others. Amongst these, $Ni(CO)_4$ and $Fe(CO)_5$ are liquid at room temperature in their stable form, and the rest of them are crystalline solids. Some of the solid carbonyl compounds exhibit congruent vaporization behavior, and others exhibit non-congruency, irrespective their molecular weight. Non-congruency is associated either direct carbonyl decomposition or disproportionation to metal/CO gas, or to metal/gas/carbonyl gas species. For example, $Co_2(CO)_8$ (M=341.95 g/mol), $Rh(CO)_{16}$ (M=1065.6 g/mol) disproportionate, whereas, $W(CO)_6$, (M= 351.92 g/mol) and $Os_3(CO)_{12}$ (M=906.7g/mol) do not disproportionate. Due to the toxicity of the above mentioned materials, safety precautions have to be taken while conducting vaporization experiments. using Knudsen cell thermogravimetric torsion effusion method, our group has performed vapor pressure measurements, on $Cr(CO)_6$, $W(CO)_6$, $Co_2(CO)_8$, $Os_3(CO)_{12}$, $Rh_6(CO)_{16}$, and $Ru_3(CO)_{12}$ in low temperature regime [7, 8].

In this paper, we report details of vaporization thermodynamics on $Re_2(CO)_{10}$ and $Ir_4CO)_{12}$ that include measuring non-equilibrium total vapor pressures (P_T) , then calculate equilibrium vapor pressure (P_e), true molecular weights of the effusing species (M), and the true fraction carbonyl decomposed (b or m_i) by the

Whitman-Motzfeldt method. In addition, we compare selected vaporization thermodynamics of the Group VIA to VIIIA metal carbonyls.

II. Experimental

Thermodynamic properties of vapors are determined by torsion effusion thermogravimetric Knudsen effusion method [9] who established a method to determine vapor pressure by using kinetic theory of dilute gases and molecular flux of the effusing gas in low pressure regimes. Specifically, we measured the total pressure exerted by vapors in a Knudsen cell (a small cylinder of a closed system with very small orifices drilled perpendicular to the wall of the cell that allows vapors to escape in form of a molecular flow in the 10^{-4} to 10^{-8} atm. regime, Concurrently, we measured the rate of weight loss of the carbonyls from the Knudsen cell, by gravimetric method that gives the molecular weights (M) of the vaporizing species at different temperatures. Details of theory of measurements are given in Margrave's book [10]. In this method, the molecular weight of the effusing species are measured by weight loss measurements [10, 11]. Using these sets of experimental data, one can calculate the equilibrium vapor pressures using Whitman-Motzfeldt method [12-13].

We will provide a general description of the apparatus in this paper. A schematic of the apparatus and procedures are given in references [14,15]. This apparatus consists of a 9 cms. diameter and ~63.5 cms. Long, one end closed, quartz tube. The other end of the quartz tube interfaces with a stainless steel flange connecting to the high vacuum system and a Cahn D100 (RH) electro-balance that is mounted on top of a frame. The high vacuum system consists of turbo molecular pump that provide vacuum levels to 10^{-7} atm. A torsion wire/mirror assembly is suspended from one arm of the Cahn balance to measure weight loss that allows calculation of molecular weights of vapors effusing from the sample during measurements. The torsion wire (in form of a fine ribbon) made of Pt-10%Ni (10-1 aspect ratio, 58.6 cm long with a torque constant of 0.0947 cm/rad.) is suspended from the balance arm to a mirror/damping disk at the bottom, that allows pressure measurements. At the bottom of the mirror assembly a long (~2 mm diameter) tungsten rod is suspended inside the quartz tube to which the Knudsen cell are attached. We used two barrel Pt-30%Rh Knudsen cells, these have small apertures (orifices) that are arranged diametrically opposite so that the vapor exerts a torque on the ribbon, which in turn gives angular motion to the mirror allowing 2θ angle measurement substituted in Eq.1. This instrument is checked for accuracies by making vapor pressure measurements on standards such as, KCl and $C_{10}H_8$. In our experiments, there was very good agreement with the measured and literature values of these standards [14].

The measurements were made using the following equations; the total pressures of the effusing gases were measured using Eq.1[16,17]

$$P_T = \frac{K.2\theta}{\sum_{i=1}^{i=n} a_i.d_i.f_i} \quad (1)$$

where P_T is the measured total pressure; K, the fiber torsion constant, torque angle, 2θ is the measured angular deflection; fi the force factor (ratio of force from the effusion of vapors from the orifices 'i' of finite wall thickness to the expected force if the orifice had an infinitesimal width) [16]; a_i the area of the orifice; d_i, the moment arm of effusion orifice; and i is the number of Knudsen cells ranging from i =1 to n, in our case n =2, [10,15].

The average measured molecular weight (M) is obtained from the thermogravimetric experiments, and the value of M is given by the Eq. 2:

$$M = 2\pi RT \left[\frac{W . \sum_{i=1}^{i=n} a_i . d_i . f_i}{K . 2\theta \sum_{i=1}^{i=n} (C . a_i)_i} \right]^2$$

$$M = \left[\sum_{i=1}^{i=n} m_i . M_i^{-1/2} \right]^{-2}$$

(2a,b)

where, $T\,(K)$ is the temperature, W is the total rate of weight loss, R is the gas constant; $m_i = b$, mass fraction of the vapor species i; and M_i is the molecular weight of the species. C_i is the orifice Clausing factor [18], and a_i = area of the orifice. Two different measurements are made using different orifice diameters. If more than one molecular species effuses out due to molecular disproportionation, then Eq. (2b) is used. Two sets of experiments on one sample, the smallest orifice diameter of the Knudsen cells is 0.06 cm, and a larger size of 0.1 cm. The Whitman-Motzfeldt equation is used to calculate the total equilibrium pressure (P_e) using Eq. 3 [12-13]:

$$P_e = P_T \left[1 + \beta \sum_{i=1}^{i=n} C_i . a_i \right] (3)$$

where, P_T is the measured total pressure from Knudsen cells with different orifice sizes; β is the cell constant for a particular cell configuration, C_i is the Clausing factor *(C)* [18], the factor $C_i\ a_i$ is related to orifice size effect, in our case, for the double barrel, i=2. Pressure equations are obtained by plotting log P_T vs.1000/T from the two orifice size Knudsen cells. In our case, for Cell #1, the pressure equation is *log* P_{T1} (atm) = B-A/T. It should be noted that the as the orifice size approaches zero the effusion pressure approaches P_e. The equilibrium, P_e is obtained by using the Whitman –Motzfeldt method by plotting $1/P_T$ vs. $\Sigma\ C_i\ a_i$. The intercept of the plot gives the $1/P_e$ and the slope gives the β/P_e. The β is related to the kinetic hindrances during the vaporization.

Equal amount of the crystalline carbonyl powders are placed in the Knudsen cells, and sealed in an argon glove box. The orifices are sealed by melting $C_{10}H_8$. The two barrels of the Knudsen cell.(~6 mm. diameter each) are welded with small plate, and attached to the tungsten rod inside the quartz tube. The d_i is the distance from the center of the plate to the orifice. A furnace is placed near the Knudsen cells. After attaining a vacuum of ~$1x10^{-7}$ atm. in the system, the sample is heated and the $C_{10}H_8$ sealing the orifices evaporates. Due to the torsion effect on the ribbon, there is a deflection in the position of the mirror that gives the 2θ angle, which is measured by using a meter scale, the values are substituted in Eq.1. In this paper, we usually measure the pressures in *atm.* then convert to *kPa*. Usually, 15-20 pressure readings are acquired at different temperatures from each orifice size Knudsen cell.

III. Results

3.1 Vaporization of solid Iridium Carbonyl - $Ir_4(CO)_{12}$

The crystalline Ir4(CO)12 exhibits canary yellow color, with MW of 1105 g/mol and melting point of 195 °C (468 K). The vaporization properties were measured using two-barrel Knudsen effusion cells, referred to as Cell #1 (orifice sizes of 0.1 cm), and Cell #2 (0.06 cm.). Results from these measurements showed a complex vaporization behavior. The measured total pressures (P_T) from the Cell #1 and #2 are listed in Table 1. The measured total pressures measured are plotted as log P_T vs.1000/T (K) in Figure 1, and the following equations are obtained:

Total vapor pressures from Cell #1

$\log P_{T1}$ (atm)=(9.516 ± 0.233)–(6393 ± 94)/T (4)

$\log P_{T1}$ (kPa)=(11.525 ± 0.234)–(6393 ± 94)/T (5)

b_1 = 0.2185 (6)

Total vapor pressures from Cell #2

$\log P_{T2}$ (atm) = (10.124 ± 0.127) – (6491 ± 52)/T (7)

$\log P_{T2}$ (kPa) = (12.130 ± 0.127) – (6491 ± 52)/T (8)

b_2 = 0.5539 (9)

It can be observed from Table 1 that the average molecular weight (M) obtained from the experiments using the weight loss measurements from Cells #1 and #2 and Eq. 2a,b. show $M^{Measured\ Cell¿}_{Ir4(CO)12(g)}1¿$ = 452 g/mol (orifice size=0.11 mm), and from Cell #2 is $M^{Measured\ Cell¿}_{Ir4(CO)12(g)}2¿$=206 g/mol (orifice size=0.06 cm). The true equilibrium molecular weight (M) of the effusing gases is 128 g/mol. However, the crystalline $Ir_4(CO)_{12}$ has a molecular weight, $M^{Theretical}_{Ir4(CO)12}$ =1106.005 g/mol. Thus, we have incongruent vaporization indicating metallic *Ir* or decomposition to another iridium gas species.

Table 1.Total pressure over solid crystalline $Ir_4(CO)_{12}$ measured by Thermogravimetric Torsion Effusion system, using two sets of Knudsen Cells. Molecular weights measured are also included.

XT1(K)	1000/ T1(K)	PT1(atm)	PT1(kPa)	log PT1(kPa)	M
Cell #1 (0.1 cm.)					
410.10	2.44	8.24E-07	8.35E-05	-4.08	696
418.50	2.39	1.70E-06	1.72E-04	-3.76	757
415.10	2.41	1.20E-06	1.22E-04	-3.91	730
418.80	2.39	1.78E-06	1.80E-04	-3.74	716
416.80	2.40	1.55E-06	1.57E-04	-3.80	620
380.50	2.63	4.53E-08	4.59E-06	-5.34	475
382.10	2.62	5.44E-08	5.51E-06	-5.26	429
397.10	2.52	2.58E-07	2.61E-05	-4.58	467
401.40	2.49	3.95E-07	4.00E-05	-4.40	456
394.40	2.54	2.64E-07	2.68E-05	-4.57	387
390.10	2.56	1.35E-07	1.37E-05	-4.86	365
405.00	2.47	5.85E-07	5.93E-05	-4.23	366
399.60	2.50	3.46E-07	3.50E-05	-4.46	366
393.30	2.54	1.88E-07	1.90E-05	-4.72	353
381.70	2.62	5.96E-08	6.04E-06	-5.22	356
414.10	2.41	1.23E-06	1.25E-04	-3.90	342
409.30	2.44	8.10E-07	8.21E-05	-4.09	325
403.50	2.48	4.98E-07	5.04E-05	-4.30	346
416.40	2.40	1.43E-06	1.45E-04	-3.84	325
419.10	2.39	1.77E-06	1.79E-04	-3.75	312
418.60	2.39	1.62E-06	1.64E-04	-3.78	303
				Av. M_1	452
Cell #2 (.06 cm)					
388.00	2.58	2.43E-07	2.46E-05	-4.61	-
400.60	2.50	8.06E-07	8.16E-05	-4.09	201

424.80	2.35	6.70E-06	6.79E-04	-3.17	257
409.20	2.44	1.97E-06	2.00E-04	-3.70	219
423.00	2.36	6.41E-06	6.50E-04	-3.19	223
427.80	2.34	9.12E-06	9.24E-04	-3.03	232
430.00	2.33	1.04E-05	1.06E-03	-2.98	213
420.80	2.38	4.76E-06	4.82E-04	-3.32	195
420.80	2.38	4.82E-06	4.88E-04	-3.31	256
391.50	2.55	3.42E-07	3.46E-05	-4.46	-
399.10	2.51	7.47E-07	7.57E-05	-4.12	151
394.30	2.54	4.49E-07	4.55E-05	-4.34	-
408.40	2.45	1.76E-06	1.78E-04	-3.75	158
408.70	2.45	1.75E-06	1.78E-04	-3.75	179
416.10	2.40	3.35E-06	3.39E-04	-3.47	183
401.60	2.49	9.56E-07	9.69E-05	-4.01	-
				Av. M_2	206

At this point, we need to know how much of the crystalline $Ir_4(CO)_{12}$ decomposed to gas, given by the b=m_i in Eq. 2b. Three possible decomposition pathways are proposed, according to Eqs. (10-12):

$Ir_4(CO)_{12}$ (s) = (1-b) $Ir_4(CO)_{12}$ (g) + b. $Ir_2(CO)_8$ + 2b. Ir (s) +4 b CO (g) (10)

2 $Ir_4(CO)_{12}$ (s) = (1-b) $Ir_4(CO)_{12}$ (g) + b. Ir_6CO_{16} + 2b. Ir (s) + 8 b CO (g) (11)

$Ir_4(CO)_{12}$ (s) = (1-b) $Ir_4(CO)_{12}$ (g) + 4 b. Ir (s) +12 b CO (g) (12)

We will use the disproportionation of $Ir_4(CO)_{12}$ (Eq. 12) and the average measured molecular weight, $M_{Ir4(CO)12}^{Exptl.Cell¿1¿}$ = 452 g/mol and $M_{Ir4(CO)12}^{Exptl.Cell¿2¿}$ = 206 g/mol, from Table 1 to calculate b values. The measured molecular weights are substituted on the left hand side of the Eq. 13 to calculate b values for each cell, ranging from 0 to 1. If b=0 only one vaporization species $Ir_4(CO)_{12}$ (g) forms, in any of the above cases shown in Eqs. 10-12. The theoretical molecular weights of the gases; $M_{Ir4(CO)12(g)}^{Theretical}$ =1106.005 g/mol,,*and* $M_{CO(g)}=28.01\,\frac{g}{mol}$ are substituted in the right hand side of the Eq.13, the unknown value b_1 = 0.2185 for Cell #1 and b_2 = 0.5539 for Cell #2 are calculated.

$$M_{Ir4(CO)12}^{Exptl.}=\left[\sum_{i=1}^{i=n} b\,x\,M_i^{\frac{1}{2}\square}\right]^{-2}=\left[\frac{(1-b)M_{Ir4(CO)12g.}^{\frac{1}{2}}+12\,b.\,M_{(CO)g}^{\frac{1}{2}}}{(1-b)M_{Ir4(CO)12.g}^{\square}+12.b.\,M_{(CO)g}^{\square}}\right]^{-2} \quad (13)$$

We also attempted to calculate the b values for Eq. 10 and 11, assuming partial decomposition to $Ir_2(CO)_8$ (g) with M = 608.52 g/mol) and $Ir_6(CO)_{16}$ (g), however, we did not find any solutions for these equations. Thus, we propose Eq.12 for the partial decomposition mechanism to $Ir_4(CO)_{12}$ (g) , Ir (s) and CO gas.

The *equilibrium* vapor pressures (P_e), true b values, and true molecular weights (M) are calculated by plotting

1/P *vs.* $\sum_{i=1}^{n} C_i . a_i$, b *vs.* $\sum_{i=1}^{n} C_i . a_i$ and M *vs.* $\sum_{i=1}^{n} C_i . a_i$, respectively, using the data obtained from the two cells. Figure 2 shows the Whitman–Motzfeldt plot for the $Ir_4(CO)_{12}$ effusion. The slope of each line plotted for different temperature in Figure 2 gives β/Peq. The average value of β =134 = (1/α.A), where α~0.012 (evaporation constant), and A= 0.63 cm^2 (cross sectional area of the Knudsen cell). The intercepts of each line give inverse *total equilibrium pressure* for $Ir_4(CO)_{12}$. An equation for (P_e) is given in Eq.14, these are also listed in Table 2.

$$\log P_e(kPa) = 12.673 - \frac{6615}{T(K)} \quad (14)$$

The true values of *b* for the vapor pressure of $Ir_4(CO)_{12}$ were also extracted by plotting *b vs.* $\sum_{i=1}^{n} C_i . a_i$, whose *intercept* gives the true value of *b*=0.6604. The plot is not shown for brevity but from the linear regression, we obtain the following equilibrium *b* value or *be* in the equation Eq.15 (note, x = slope of the line):

$$b_e = 0.6604 - 19.8\ x \quad (15)$$

In a similar manner the true values of the molecular weights (M) of the effusing gas were obtain by plotting M *vs.* $\sum_{i=1}^{n} C_i . a_i$ as shown in Figure 3. The *intercept* gives the true M =128 g/mol for the decomposition of $Ir_4(CO)_{12}$.using Eq.16 (note , x= slope of the line):

$$M_e = 127.89 - 14523\ x \quad (16)$$

The measured P_{T1} and P_{T2} measured from Knudsen cells with different orifices and the calculated P_e at different temperatures are tabulated in Table 2.

Table 2. The measured total pressures (P_{T1} and P_{T2}) and the calculated equilibrium pressures (P_e) from the intercept (1/Pe) of the Whitman-Motzfeldt plot for the reaction Ir4(CO)12(s) =(1-b) Ir4(CO12 (g) +4 b.Ir (s) +12 b.CO(g).

T (K)	P_{T1}(atm)	P_{T2}(atm)	$1/P_e$ (atm^{-1})	P_e (atm)	P_e (kPa)
380	4.9374 x10^{-8}	1.1034 x10^{-7}	5.5094 x10^{6}	1.815 x10^{7}	1.839 x10^{-5}
390	1.3330 x10^{-7}	3.0249 x10^{-7}	1.9735 x10^{6}	5.067 x10^{-7}	5.134 x10^{-5}
400	3.4247 x10^{-7}	7.8850 x10^{-7}	7.4376 x10^{5}	1.345 x10^{-6}	1.362 x10^{-4}
410	8.4026 x10^{-7}	1.9615 x10^{-6}	2.9380 x10^{5}	3.404 x10^{-6}	3.449 x10^{-4}
420	1.9753 x10^{-6}	4.6722 x10^{-6}	1.2124 x10^{5}	8.248 x10^{-6}	8.357 x10^{-4}
430	4.4628 x10^{-6}	1.0689 x10^{-6}	5.2111 x10^{4}	1.919 x10^{-5}	1.944 x10^{-3}

The partial pressures of $Ir_4(CO)_{12}$ (g) and the CO gas, are determined by Eq. 17 and 18 for the reaction in Eq.12 by substituting, *b*=0.6604; $P_{Ir_4(CO)_{12}}/P_e$ = 0.21207 for the $Ir_4(CO)_{12}$ (g), and for the iridium metal formation with the evolution of carbon monoxide gas, $P_{CO_{\square}}/P_e$ = 0.7879.

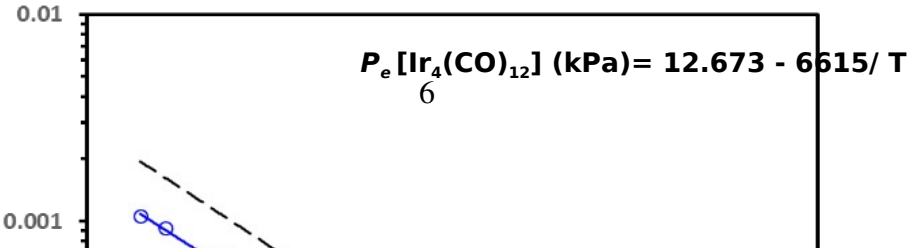

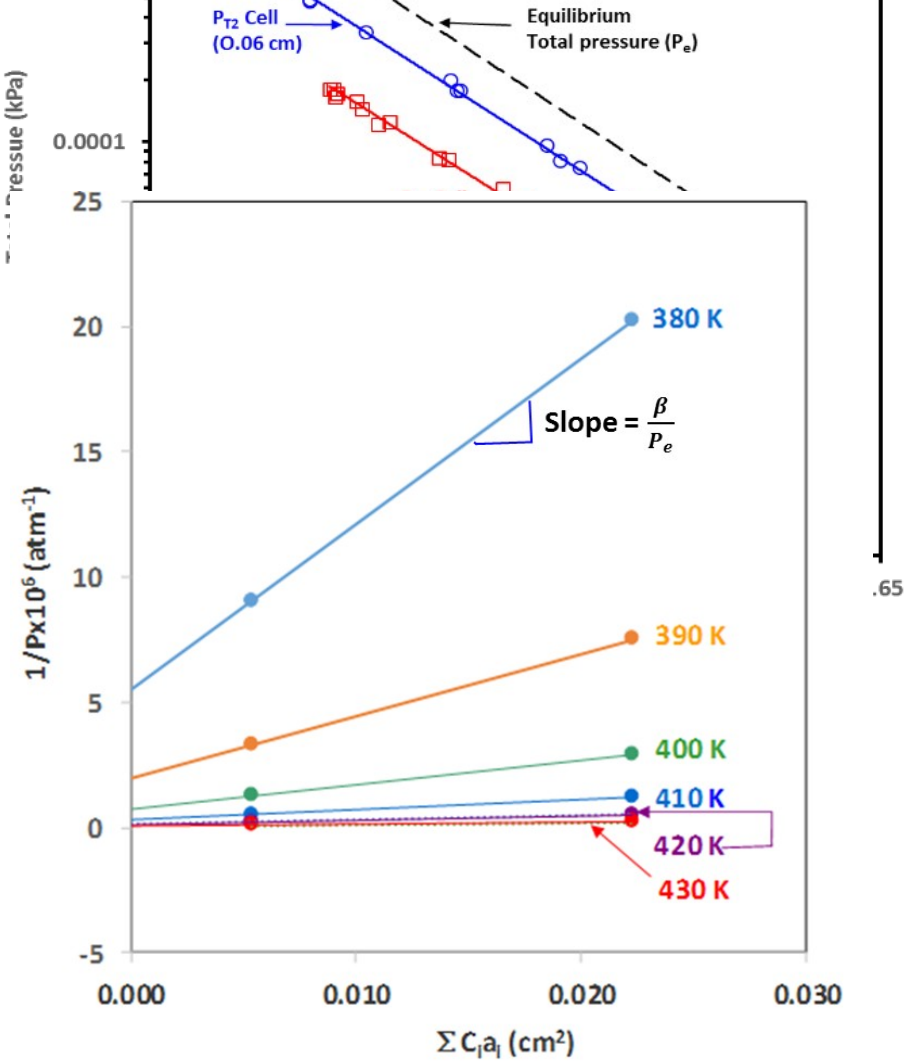

Figure 2. Whitman–Motzfeldt plot for $Ir_4(CO)_{12}$ showing the effect of orifice size and temperature

on the equilibrium pressures. (Cell #1, orifice size, 0.1 cm and $\sum_{i=1}^{n} C_i . a_i = 0.022318$, and for Cell #2, orifice size 0.06 cm., and $\sum_{i=1}^{n} C_i . a_i = 0.0053788$. The equilibrium pressure is given by the intercepts at each temperature.

$$\frac{P_{Ir4|C|12(g)}}{\left[\frac{(1-m_i)M^{\frac{1}{2}}_{Ir4|CO|12g.}}{}\right]^{\square}} = 0.21207$$

The partial pressures at different temperatures are tabulated in Table 3 along with total equilibrium pressures (P_e) between 380 and 430K. From the total equilibrium vapor pressure (P_e) and the *b* value, we calculated, the partial pressure of the $Ir_4(CO)_{12}$ (g) and CO gas (Eqs. 17, 18) and the equilibrium constant, K_P for each vaporization reaction. The solid-gas equilibrium for the $Ir_4(CO)_{12}$ (Eq. 19) is represented as :

$Ir4(CO)_{12}$ (s) = $Ir_4(CO)_{12}$ (g) (19)

Table 3. Partial pressures of $P_{Ir4(CO)12}$ and P_{CO} as a function of temperature for the reaction $Ir_4(CO)_{12}$ (s) = (1-*b*) $Ir_4(CO)_{12}$ (g) + 4 *b*.Ir (s)+ 12 *b* CO (g)

Temp. (K)	1/T (1/K)	Equilibrium Pressure (P_e) (kPa)	Partial Pressures (kPa) $P_{Ir4(CO)12}$	P_{CO}
380	2.632×10^{-3}	1.839×10^{-5}	3.900×10^{-6}	1.449×10^{-5}
390	2.564×10^{-3}	5.134×10^{-5}	1.089×10^{-6}	4.045×10^{-5}
400	2.500×10^{-3}	1.362×10^{-4}	2.888×10^{-5}	1.073×10^{-4}
410	2.439×10^{-3}	3.449×10^{-4}	7.314×10^{-5}	2.718×10^{-4}
420	2.381×10^{-3}	8.357×10^{-4}	1.772×10^{-4}	6.585×10^{-4}
430	2.326×10^{-3}	1.944×10^{-3}	4.123×10^{-4}	1.523×10^{-3}

Using the equilibrium constant, $K_{p\,(\text{Eq. 19})} = P_{\text{Ir4CO12 (s)}} = 0.21207\ P_{e.}$ (20)

The Gibbs energy change ($\Delta G^o = -RT\ln Kp$,) for the reaction (Eq.19) is determined by using Eq. 20 as follows from the plot in Figure 3(a) :

$\Delta G^o_{Eq.19} = 126.7 - 0.2298\ T$ (kJ/mol)
(21)

Eq. 22 gives the decomposition of the iridium carbonyl to metallic Ir and CO gas, from the plot in Figure 3(b):

Ir_4CO_{12} (s) = 4 Ir (s) + 12 CO (g) (22)

For which, $K_p = P_{CO}^{12} ¿ (0.7879\,P_e)^{12}$ (23)

The Gibbs energy change for the reaction (Eq. 22) is determined as follows:

$\Delta G^o_{Eq.22} = 2000 - 2.888T$ (kJ/mol) (24)

Thus, using the Knudsen cell and Whitman–Motzfeldt methodology it is possible to determine the equilibrium thermodynamic properties of $Ir_4(CO)_{12}$.

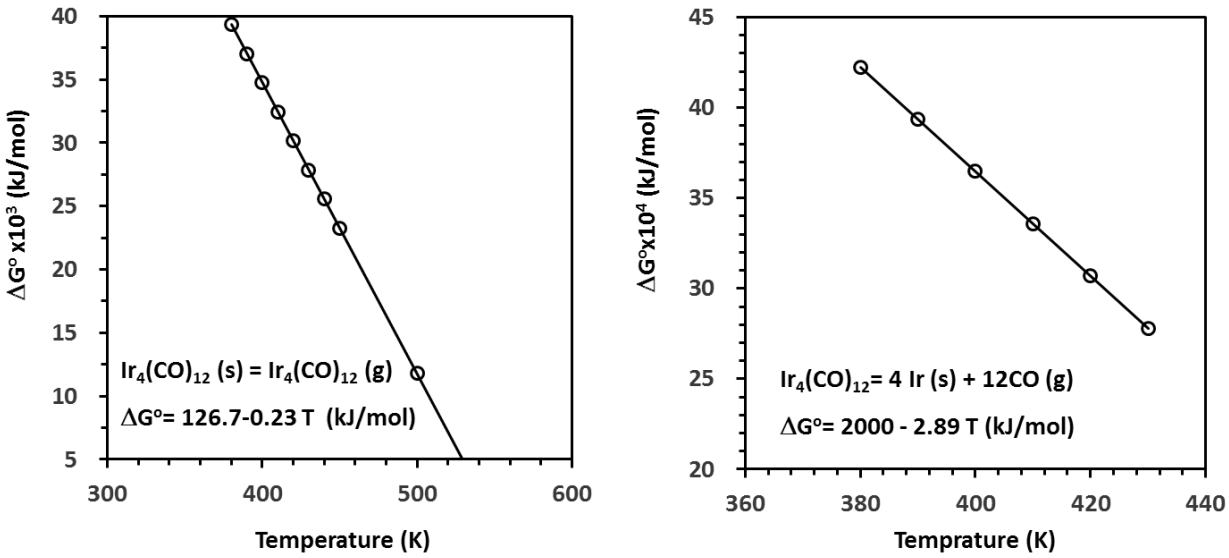

Figure 3 (a) Equilibrium Gibbs energies for solid–gas Ir4(CO)12 of Eq. 19, Figure 3(b) shows decomposition Gibbs energies according to the Eq. 22.

3.2 Vaporization behavior of $Re_2(CO)_{10}$

The vapor pressure measurements for crystalline $Re_2(CO)_{10}$ (s), that exhibit white color, with MW of 625.5 g/mol and melting point of 170°C (443K), were also measured in a similar manner as those for $Ir_4(C0)_{12}$, but the results obtained were quite different as compared to $Ir_4(CO)_{12}$ in terms of orifice size dependence. There was negligible orifice size effect similar that obtained in the vaporization of KCl(s). The $Re_2(CO)_{10}$ did not decompose to Re metal nor particulate soot was observed in the quartz glass tube during the vaporization experiments of $Re_2(CO)_{10,}$ in the temperature range of 298K to 320K. The equilibrium vaporization of $Re_2(CO)_{10}$ is given by the following equation:

$$Re_2(CO)_{10}(s) = Re_2(CO)_{10}(g) \quad (25)$$

The measured vapor pressure data from solid $Re_2(CO)_{10}$ (s) using two different orifice sizes are shown in Table 4 and plotted in Figure 4, indicating virtual congruency.

Total Vapor pressure using Cell #1

$$\log P_{T1}\,(atm) = 9.283 - 4745.3/T\,(K) \quad (26)$$

$$\log P_{T1}\,(kPa) = 11.288 - 4745.3/T\,(K) \quad (27)$$

Total vapor pressures from Cell #2

$$\log P_{T2}\,(atm) = (10.392 \pm 0.092) - (5089.7 \pm 28)/T \quad (28)$$

$$\log P_{T2}\,(kPa) = (12.397 \pm 0.092) - (5089.7 \pm 28)/T \quad (29)$$

Figure 4. Measured total vapor pressure of $Re_2(CO0_{10}$ using two Knudsen cells with different orifices sizes, designated as P_{T1} and P_{T2} . The total equilibrium vapor pressure (*Pe*), shown as dotted line is calculated using Whitman–Motzfeldt method..

Table 4. Total pressure over solid crystalline $Re_2(CO)_{10}$ measured by Thermogravimetric Torsion Effusion system, using two sets of 2-Barrel Knudsen Cells with different orifice sizes of 0.1 cm (Cell #1) and 0.06 cm (Cell #2).

T (K)	1000/ T	P_T (atm)	P_T (kPa)	logP_T (kPa)	MW(g/ mol)
Cell #1 (0.1 cm.)					
302.17	3.31	3.54×10^{-7}	3.59×10^{-5}	-4.45	-
321.50	3.11	3.55×10^{-6}	3.60E-04	-3.44	787
321.65	3.11	3.68×10^{-6}	3.73E-04	-3.43	795
324.90	3.08	5.47×10^{-6}	5.54E-04	-3.26	795
325.69	3.07	5.90×10^{-6}	5.97E-04	-3.22	782
329.35	3.04	8.60×10^{-6}	8.72E-04	-3.06	806
329.35	3.04	8.56×10^{-6}	8.67E-04	-3.06	817
331.00	3.02	1.06×10^{-6}	1.07E-03	-2.97	827
330.10	3.03	9.13×10^{-6}	9.25E-04	-3.03	820
309.51	3.23	8.99×10^{-7}	9.11E-05	-4.04	775
307.91	3.25	7.33×10^{-7}	7.43E-05	-4.13	804
316.87	3.16	2.18×10^{-6}	2.21E-04	-3.66	791
311.75	3.21	1.15×10^{-6}	1.17E-04	-3.93	791
309.70	3.23	8.71×10^{-7}	8.82×10^{-5}	-4.05	813
				Av. M_1	800
Cell #2 (.06 cm)					
298.53	3.35	2.48×10^{-7}	2.51×10^{-5}	-4.60	670
298.70	3.35	2.52×10^{-7}	2.55×10^{-5}	-4.59	693
313.83	3.19	1.50×10^{-6}	1.52×10^{-4}	-3.82	704
314.95	3.18	$1.69 \times 10^{-}$	1.72×10^{-4}	-3.77	727

		1.82×10^{-6}			
315.75	3.17	1.84×10^{-4}	-3.73	776	
		2.72×10^{-7}			
299.71	3.34	2.76×10^{-5}	-4.56	657	
		2.73×10^{-7}			
299.71	3.34	2.77×10^{-5}	-4.56	663	
		2.23×10^{-6}			
318.10	3.14	2.26×10^{-4}	-3.65	731	
		2.55×10^{-6}			
319.17	3.13	2.59×10^{-4}	-3.59	761	
		3.02×10^{-7}			
300.19	3.33	3.06×10^{-5}	-4.51	615	
		3.10×10^{-7}			
300.35	3.33	3.14×10^{-5}	-4.50	664	
		5.85×10^{-7}			
305.81	3.27	5.92×10^{-5}	-4.23	657	
		6.95×10^{-7}			
307.27	3.25	7.04×10^{-5}	-4.15	725	
		1.10×10^{-6}			
311.27	3.21	1.12×10^{-4}	-3.95	734	
		2.30×10^{-6}			
318.10	3.14	2.33×10^{-4}	-3.63	775	
		2.27×10^{-6}			
317.94	3.15	2.30×10^{-4}	-3.64	781	
		4.75×10^{-7}			
304.45	3.28	4.82×10^{-5}	-4.32	-	
		2.75×10^{-7}			
299.55	3.34	2.79×10^{-5}	-4.55	652	
			Av. M_2	705	

The Whitman-Motzfeldt plot (1/P vs. $\sum_{i=1}^{2} C_i . a_i ¿$, not shown, were made from the measured total vapor pressures (Eqs. (26) and (28)). The equilibrium vapor pressures are shown in Table 5 and plotted in Figure 4 . The $b = 0$ as well as the β=0. The equation for the equilibrium total vapor pressure is calculated as follows:

$$\log P_e \text{ (kPa)} = 9.396 - 4167/T(K) \quad (30)$$

The extrapolated true M = 675 (g/mol) which is closer to the theoretical value (within experimental error), as compared to the measured M (Cell#1) = 800 g/mol, and from Cell No.2= 705 g/mol. From Table.

Using the equilibrium constant, $K_p = P_{Re2(CO)10}$, (b = 0), the Gibbs energy change for the vaporization is obtained represented by the following Eq. (31) which is obtained by plotting Figure 5:

$$\Delta G^o \text{ (kJ/mol)} = 80.0 - 0.180\ T \quad (31)$$

Table 5. Total equilibrium pressure (P_e) extracted by using Whitman Motzfeldt solid $Re_2(CO)_{10}$ model using Cell #1 (0.1 cm) and Cell #2 (0.06 cm) orifice diameter Knudsen cells.

T (K)	1000/ K	1/Pe (atm)	Pe (atm)	Pe (kPa)	log (kPa)
290	3.45	**T (K)**	1.00E-07	1.01E-05	-4.9943
300	3.33	290	3.33E-07	3.38E-05	-4.4714
310	3.23	300	1.00E-06	1.01E-04	-3.9943
320	3.13	310	2.81E-07	2.85E-05	-4.545
330	3.03	320	7.83E-06	7.94E-04	-3.1003

340	2.94	330	2.05E-05	2.07E-03	-2.6831

IV. Discussion

The vaporization behavior solid carbonyls in Group VIA to VIIIA (in Table 6) ; Mo (42), Ru (44), Rh (45),W(74), Re (75), Os(76) and Ir (77) are compared with $Ir_4(CO)_{12}$ (M = 1105.6 g/mol) and $Re_2(CO)_{10}$ (M= 625.5 g/mol). Our measurements were made at lower temperatures and pressures using thermogravimetric torsion effusion Knudsen cell method, and the data for the higher temperature is from the literature. Table as shown in the Table 6.

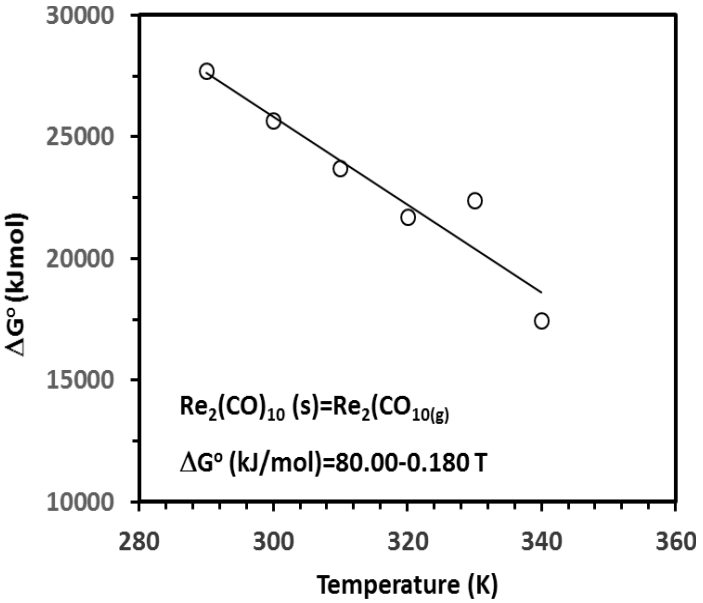

Figure 5 Equilibrium Gibbs energies for solid–gas Ir4(CO)12 of Eq. 25.

Table 6. Group VIA ,VIIA and VIIIA listing of solid carbonyl compounds

Group	*6* *Group VIA*	*7* *Group VIIA*	*8* *Group VIIIA*	*9* *Group VIIIA*
Element/Carbonyl	Mo 42- $Mo(CO)_5$ M= 264.01 g/mol	Tc 43 (not studied)	Ru 44 - $Ru_3(CO)_{12}$ M= 639.33 g/mol	Rh 45- $Rh_6(CO)_{16}$ M= 1065.6 g/mol
Atomic Number/ Molecular Weight	W 74- $W(CO)_6$ M=351.92 g/mol	Re 75- $Re_2(CO)_{10}$ M= 632.71 g/mol	Os 76-$Os_3(CO)_{12}$ M= 906.7 g/mol	Ir 77- $Ir_4(CO)_{12}$ M=1105.01 g/mol

4a. *Group VIA (W and Mo carbonyls)*

The vapor pressure data in the low temperature regime of $W(CO)_6$ showed congruent vaporization and the equilibrium pressure and Gibbs energy are shown Eqs. 32 to 34 [7] :

$$W¿)\,(s) = W¿)\,(g) \tag{32}$$

$$\log P_T(kPa)_{W(CO)_6} = 11.098(0.11) - \frac{4060(31)}{T(K)} \tag{33}$$

$$\Delta G^o_{Eq.34} = 77{,}714 - 173\,T\ kJ/mol \tag{34}$$

The high temperature vapor pressure measurements on $W(CO)_6$ were reported by Baev [19], Windsor and Blanchard [20], Hieber and Romberg [21], Ginsburg [22] and Lander and Germer [6]. The data from Rezzukhina and Shvyrev [23] is given by the Eq.35 in the range of 338.76 to 410.13 K:

$$\log P\ (\text{kPa}) = 10.072 - 3640.4/T \tag{35}$$

We did not perform any experiments on vaporization of $Mo(CO)_6$, but we included the values of Rezzukhina and Shvyrev [23] in the range of 323.68 K to 402.77 K

$$\log P \text{ (kPa)} = 10.8522 - 3788.3/T \quad (36)$$

Figure 6 shows vapor pressures of all the relevant carbonyls for comparison purposes.

4b.. Group VIIA (Re Carbonyl)

The low temperature data from this study on $Re_2(CO)_{10}$ showed congruent vaporization, and equilibrium vapor equation is given in Eq. 30. The higher temperature data on $Re_2(CO)_{10}$ were first published in 1961 by Ginzburg [22], Eq. (37), in the range of 351K to 408.5K. In 1971, Baev et al. [25] published equations, in the range of 356K to 454K, Eq. (38) for the crystal-vapor equilibrium in Eq.25:

$$\log P \text{ (kPa)} = 9.808 - 4152/T \text{ (K)} \quad (37)$$

$$\log P \text{ (kPa)} = 9.6558 - 4054.6/T \text{ (K)} \quad (38)$$

4c. Group VIIIA (Ru, Os, Rh, and Ir Carbonyls)

Thermodynamic vaporization properties of Ru, Rh and Ir carbonyls show disproportionation effects, with the exception of $Os_3(CO)_{12}$. Our previous vapor pressure studies [24] showed congruent vaporization, and the equilibrium is represented as Eq.39 :

$$Os_3(CO)_{12} \text{ (s)} = Os_3(CO)_{12} \text{ (g)} \quad (39)$$

$$\log P_{e\ Eq.xx} = 15.00 - 7101/T \text{ (K)} \quad (40)$$

$$K_{Pe\ Eq.39} = [1x\ P_{Os3(CO)12}] = [\ 1\ x\ (15.00 - 7101/T(K)] \quad (41)$$

$$\Delta G^{o}_{Eq.\ 39} \text{ (kJ/mol)} = 134.2 - 0.021\ T(K) \quad (42)$$

Gaidym et al. [26] only reported an pressure equation for $Os_3(CO)_{12}$ between 423 to 543 K in Eq. 43:

$$\log P_e \text{ (kPa)} = 14.792 - 5659/T \text{ (K)} \quad (43)$$

The high temperature data of Giadym et al. [26] does not agree with our results, at this point we cannot comment with regards to the discrepancy without performing experiments. Although, we performed Onnk's OAR analyses showed that the data does not follow the arc representation in our thermodynamic assessment paper [27].

In similar temperature ranges, the $Ru_3(CO)_{12}$ with MW of 639.3 (g/mol) and partially disproportionates to metallic Ru, between 314 and 352K. The solid-gas equilibrium is extracted is given below [24]:

$$Ru_3(CO)_{10} \text{ (s)} = Ru_3(CO)_{10} \text{ (s)} \quad (44)$$

$$\log P_{e\ Eq.44} = 12.51 - 5392/T \text{ (K)} \quad (45)$$

$$K_{Pe\ Eq.44} = [0.215\ x\ P_{Ru3(CO)10}] = [0.215\ x\ (12.51 - 5392/T\ (K)] \quad (46)$$

$\Delta G^{o}_{Eq.\ 44}$ (kJ/mol) = 103.2 - 0.214 T(K) (47)

The decomposition portion of it is represented by the equation [24]:

$Ru_3(CO)_{10}$ (s) = 3. Ru (s) + 12CO (g) (48)

$K_{Pe\ Eq.48}$ (kPa) = [0.785 x $P_{Ru3(CO)10}$]^{12} = [0.785 x (12.51 - 5392/T (K)]^{12} (49)

$\Delta G^{o}_{Eq.\ 48}$ (kJ/mol) = 1237.8 – 2.39 T(K) (50)

The $Rh_6(CO)_{16}$ completely disproportionates and decomposes to metallic Rh and CO gas, in the range of 320 to 370 K [7, 28]. We extracted the Rh metal crystals and performed line broadening x-ray diffraction that showed very broad Bragg peaks, and extremely fine crystallite sizes in the order of Deff~46 Å were measured [29]. The following are the equations for vaporization of $Rh_6(CO)_{16}$ (s) [8,28,29]:

$Rh_6(CO)_{16}$ (s) = 6.Rh (s) + 16 (CO) (g) (51)

$\log P_{e\ Eq.51}$ = 12.533 - 5540/T(K) (52)

$K_{Pe\ Eq.51}$ = [1 x $P_{Rh6(CO)16}$]^{16} = [1x (12.51 - 5392/T (K)]^{16} (53)

$\Delta G^{o}_{Eq.\ 51}$ (kJ/mol) = 1697.1 – 3.23 T(K) (54)

In summary, the determination of equilibrium vaporization thermodynamics of crystalline $Ir_4(CO)_{12}$ (M=1105.6 g/mol) equations and $Re_2(CO)_{10}$ (M=625.5 g/mol) in this study revealed incongruent vaporization of $Ir_4(CO)_{12}$ and congruent vaporization of $Re_2(CO)_{10}$. To the best our knowledge, we could not find vaporization data on $Ir_{4(}CO)_{12,}$ however, we found data on $Re_2(CO)_{10}$.at higher temperatures.

Figure 6 shows comparative data of carbonyls summarized the data from the literature. The vapor pressure with lines with data points are from present and previous studies our group, and ones with only lines are from the literature. As the measurements were made in high vacuum, our pressure range is between ~1x10^{-6} to ~1x10^{-3} kPa. High pressure and temperature data is from the literature ranging from ~2x10^{-4} to ~200 kPa.

Extrapolation of the pressure data, discussed above, at 300K (Figure 6), showed that the VIA group Mo and W carbonyls have higher vapor pressures than those of Group VIIA, Re carbonyl, and VIIIA, Ru, Os, Rh, and Ir carbonyls. The equilibrium Gibbs energy functions derived in this study are compared with those of the previously investigated carbonyls and these results are shown in Figure 7. In general, the ΔG^{o} of solid to gas equilibrium of the Ir, Os, Ru, and Re carbonyls were lower than those of carbonyls that decomposed to metal and carbon monoxide gas.

V. Conclusions

Vaporization thermodynamic measurements, using gravimetric torsion-Knudsen effusion method, of Os, W, Cr, Rh, Ru, Co showed equilibrium vapor (Pe) dependence on molecular weights at a particular temperature. Overall, there is reasonable agreement between low temperature studies from our group with studies performed at higher temperature reported in the literature except for the $Os_3(CO)_{12}$. Amongst the high molecular weight carbonyls, the $Rh_6(CO)_{16}$, $Ru_3(CO)_{12}$ and $Ir_4(CO)_{12}$ exhibited disproportionation. Whereas, the $Re_2(CO)_{10}$ and $Os_3(CO)_{12}$ showed congruent vaporization without any disproportion in the temperature of the studies. Extrapolating the total vapor pressure data to room temperature, we conclude that the vapor pressure of various crystalline carbonyls show that total equilibrium pressure (Pe) follow the trend below:

Vapor Pressure: $P_{e\ Mo(CO)6} > P_{e\ W(CO)6} > P_{e\ Re2(CO)10} > P_{e\ Ru3(CO)12} > P_{e\ Rh6(CO)16} > P_{e\ Os3(CO)12} > P_{e\ Ir4(CO)12}$

M (g/mol):	264.01	351.92	632.71	639.32	906.7	1065.6	1106.5

Equilibrium Gibbs energies for decomposition vaporization to metal and CO gas are much higher than for the solid-gas carbonyls reactions.

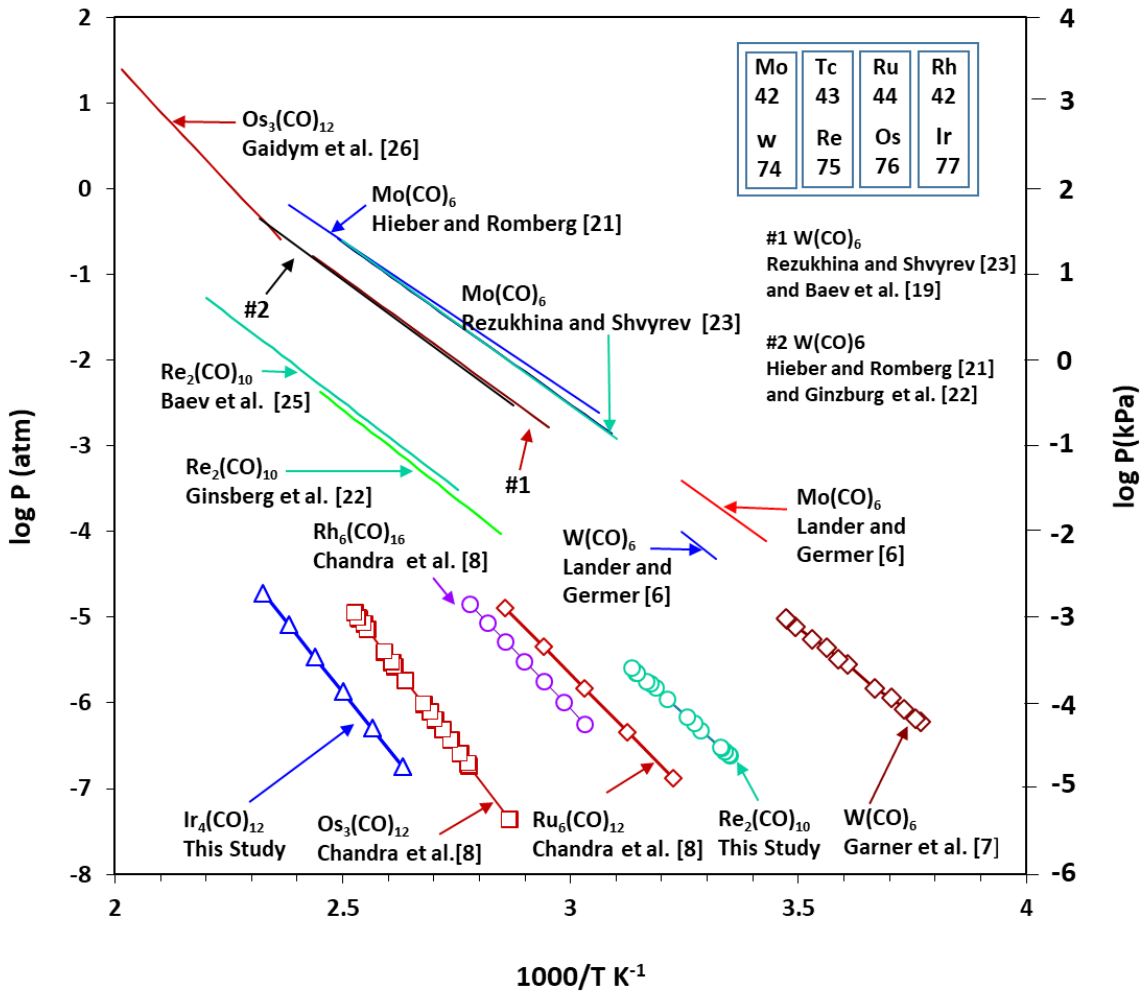

Figure 6. Comparison of total vapor pressures of group VIA to VIIIA carbonyls. The Ir4(CO012 and Re2(CO)10 plots are from this study.

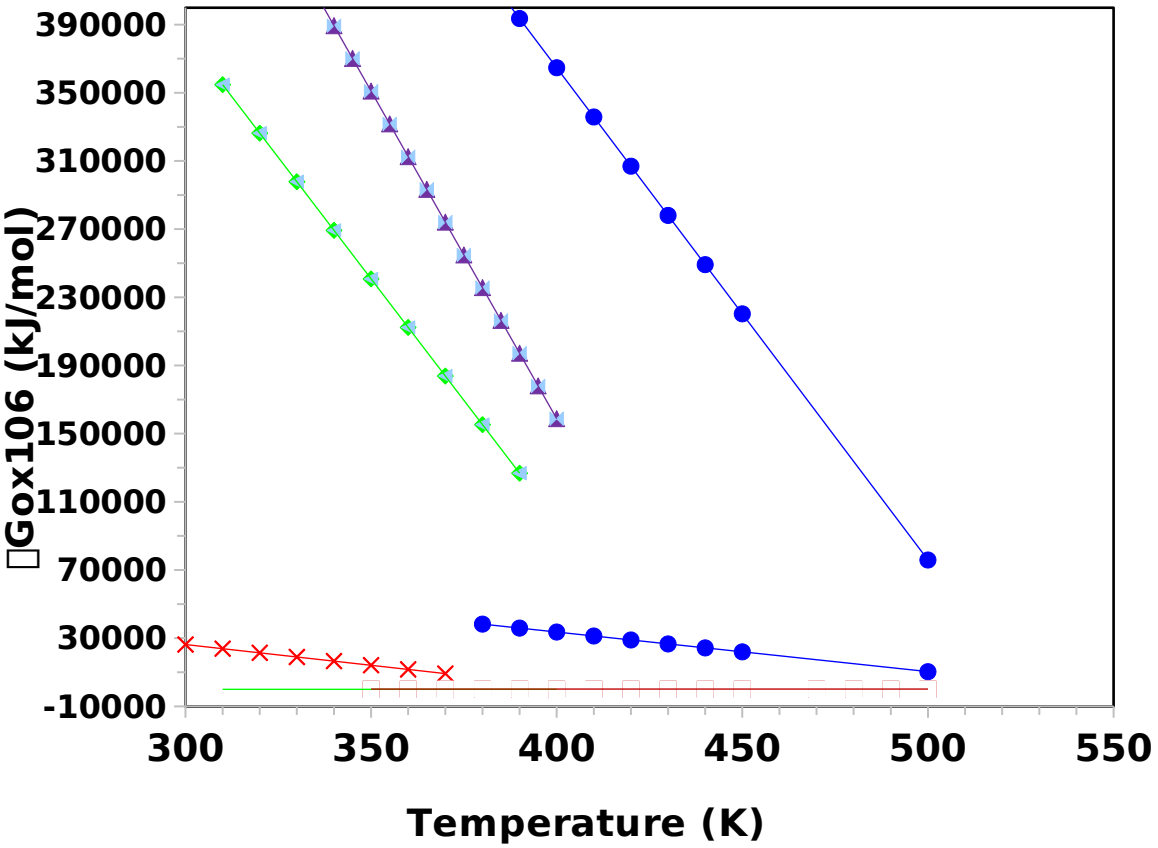

Figure 7. Comparison of equilibrium and decomposition Gibbs energies of Ir, Os, Ru, and Re carbonyls.

Acknowledgements

The authors would like to acknowledge the financial support of National Science Foundation (NSF: Grant No. 0132556), and earlier support of US Bureau of Mines (USDI G1145229 3271) through University of Missouri, Rolla. We also thank Prof. Dennis Lindle of University of Nevada, Las Vegas for his support for the project. One of us (D. Chandra), acknowledge the support of the Molecular Foundry, Lawrence Berkeley National Laboratory, DOE.

References

References

1. H.W. Pfeifer, Hybrid and Selected Metal Matrix Composites, Chapter 6, 1. Renton, Ed, AIAA, 12900 Avenues of Americas, NY, 1977.
2. D. Chandra, J.D. Mote, P.K. Predecki, A feasibility study of Ni carbonyl CVD coatings for graphite aluminum composites, J Report US, U.S. MERADCOM, Fort Belvoir, 1982, USDOD Contract No.DAAK-70-81-C-0035, 1982.

3. D. Chandra, J.D. Mote, P.K. Predecki, A feasibility study of zone melting methods for the fabrication of Al-graphite to U.S.MERADCOM, USDOD Contract No. DAAK-70—82-C-0140, 1985.
4. M.Kh. Shorovshrov, et al., *Adgez. Rasplavav-Packa Mater*. 1 (1976) (Chem. Abst. (ref. 88:10627P,1978) (1978)).
5. M.Kh. Shorovshro, Ftz. Khim, *AbnuLMater.* 4 (1976) 141–143, (Metals Abstract (1976)).
6. J.J. Lander, L.H. Germer, Technical Publication #2259, *AIME, Inst. of Metals Division, Metals Technology* (London), 71, 459 and 487, 1947, pp. 1-41.
7. M.L. Garner, D. Chandra, K.H. Lau, *J. Phase Equilib.* **16**(1) (1995), 24-29.
8. D. Chandra, M.L. Garner, K.H. Lau, *J. Phase Equilib*. **20**(6) (1999), 565-572.
9. M. Knudsen, Effusion and Molecular flow of gases through openings, *Ann. Physik.*, **28**, 1909, 999.
10. J. Margrave, *Characterization of High Temperature Vapors*, John Wiley, New York, 1967., also see the article by R.D. Freeman, The characterization of high temperature vapors," , 152-192, in this book.
11. D. L. Hildenbrand and D.T. Knight, Vaporization of behavior of Boron Nitride and Aluminum Nitride , J. *Phys. Chem*.**43**, 1963, 888-893.
12. C. I. Whitman, The measurement of vapor pressure by effusion, J. *Chem*. Phys., **20**, 1952, 161-166.
13. K. Motzfeldt, The thermal decomposition of sodium carbonate by the effusion method, , *J. Chem*. Phys., **59**, 1955, 139- .
14. Dhanesh Chandra, K.H. Lau, Wen-Ming. Chien, and Michael Garner *J. Phys. Chem*. **66** (2005), 241-245.
15. M. Garner, *Vapor pressures and thermodynamics properties tungsten, chromium, cobalt and rhodium carbonyls*, MS Thesis, University of Nevada, Reno, 1994.
16. A.W. Searcy and R.D. Freeman, Determination of molecular weights of Vapor at high temperatures I. The Vapor Pressure of Vapor at high temperatures, *J. Am. Ceramic Soc.* 76, 1954, 5229.
17. R.D. Freeman and A. W. Searcy, The effect of channel holes on the Force exerted by effusing vapors, J. Chem. Phys. 22, 1954, p762.
18. P. Clausing, The flowing of very dilute gases through tubes of any length. *Ann. Physik*. 12, 1932, 961.
19. A.K. Baev, V.V. Dem'yanchuk, *Obshch. Prikl. Khim*. 2 (1970)167–176.
20. L.M. Windsor, A.A. Blanchard*, J. Am. Chem. Soc*. 56 (1934) 823.
21. W. Hieber and E. Romberg, Z. *Anorg. Allg. Chem.* 221 (1935), 332-336.
22. A.A. Ginzburg, *Zh. Prikl. Khim*. 34 (1961), 2569.
23. T.N. Rezzukhina, V.V. Shvyrev, 7(No. 6 *Ser. Fiz.-Mat. i Estestven. Nau* No. 4) (1952), 41-46.
24. Dhanesh Chandra, K.H. Lau, Wen-Ming. Chien, and Michael L Garner *J. Phys. And Chem*,. 66 (2005), 241-245.
25. A.K. Baev, N.A. Belozerskii, O.D. Krichevskaya, *Obsh. Prikl. Khim*., 2 (1970), 161-176.
26. I.L. Gaidym, A.K. Baev, V.G. Syrkin, A.A. Uelskii, A.V. Medvedeva, *Zh. Fiz. Khim*. 48(7) (1974), 1871.
27. Raja Chellappa, and Dhanesh Chandra, The Journal of Chemical Thermodynamics 37(4):377–387
28. M. Garner, *Vapor pressures and thermodynamics properties tungsten,chromium, cobalt and rhodium*

carbonyls, MS Thesis, University of Nevada, Reno, 1994.

29. D. Chandra, H. Mandalia, M.L. Garner, K.H. Lau, and M.K. Blakeley, *Advances in X-ray Analyses* (1995), 413-425.